A TRPC6-dependent pathway for myofibroblast transdifferentiation and wound healing in vivo

Jennifer Davis[1], **Adam R. Burr**[1], **Gregory F. Davis**[1], **Lutz Birnbaumer**[3], and **Jeffery D. Molkentin**[1,3,*]

[1]Department of Pediatrics, University of Cincinnati, Cincinnati Children's Hospital Medical Center, Cincinnati, Ohio, 45229, USA

[2]Howard Hughes Medical Institute, Cincinnati, Ohio, 45229, USA

[3]Laboratory of Neurobiology, National Institute of Environmental Health Sciences, National Institutes of Health, Research Triangle Park, NC 27709, USA

Summary

After injury or cytokine stimulation, fibroblasts transdifferentiate into myofibroblasts, contractile cells that secrete extracellular matrix for wound healing and tissue remodeling. Here, a genome-wide screen identified TRPC6, a Ca^{2+} channel necessary and sufficient for myofibroblast transformation. TRPC6 overexpression fully activated myofibroblast transformation, while fibroblasts lacking *Trpc6* were refractory to transforming growth factor-β (TGFβ) and angiotensin II-induced transdifferentiation. *Trpc6* gene-deleted mice showed impaired dermal and cardiac wound healing after injury. The pro-fibrotic ligands TGFβ and angiotensin II induced TRPC6 expression through p38 mitogen-activated protein kinase (MAPK) - serum response factor (SRF) signaling via the TRPC6 promoter. Once induced, TRPC6 activates the Ca^{2+}-responsive protein phosphatase calcineurin, which itself induced myofibroblast transdifferentiation. Moreover, inhibition of calcineurin prevented TRPC6-dependent transdifferentiation and dermal wound healing. These results demonstrate an obligate function for TRPC6 and calcineurin in promoting myofibroblast differentiation, suggesting a comprehensive pathway for myofibroblast formation in conjunction with TGFβ, p38 MAPK and SRF.

INTRODUCTION

Fibroblast to myofibroblast conversion plays a critical role in wound healing and tissue remodeling after injury (Hinz, 2007; Tomasek et al., 2002). Myofibroblasts synthesize extracellular matrix (ECM) components and generate high contractile forces for wound retraction or tissue remodeling in developmental processes (Hinz, 2007). However,

Publisher's Disclaimer: This is a PDF file of an unedited manuscript that has been accepted for publication. As a service to our customers we are providing this early version of the manuscript. The manuscript will undergo copyediting, typesetting, and review of the resulting proof before it is published in its final citable form. Please note that during the production process errors may be discovered which could affect the content, and all legal disclaimers that apply to the journal pertain.

See online supplement for a full listing of the experimental procedures.

SUPPLEMENTAL INFORMATION

Supplementary information includes 3 figures and an Extended Experimental Procedure section, and can be found with this article online at:

Conflict of interest: None (no competing financial interests).

persistent myofibroblast activity can underlie hypertrophic scarring, loss of tissue compliance, and even rampant fibrosis that is the basis for fibrotic disorders of the heart, skin, lung, kidney, skeletal muscle and liver (Hinz, 2007; Wynn, 2008). The myofibroblast is considered a hybrid cell type with both smooth muscle and fibroblast qualities (Hinz, 2007). A defining feature of myofibroblast differentiation is the formation of smooth muscle α-actin (αSMA) stress fibers that provide a structural network for generating contractile forces (Hinz, 2007; Tomasek et al., 2002). Myofibroblasts synthesize ECM proteins including collagen and a specialized fibronectin splice variant Fn-ED-A (Serini et al., 1998; Tomasek et al., 2002).

During acute tissue injury mesenchymal and inflammatory cells secrete profibrotic cytokines and chemokines such as transforming growth factor β (TGFβ), angiotensin II (AngII), connective tissue growth factor and endothelin-1 (ET-1) to induce or augment myofibroblast transformation (Derynck and Zhang, 2003; Leask, 2010). TGFβ signals through a heterodimeric receptor at the plasma membrane in which a TGFβ type 2 receptor (TGFBR2) activates a TGFβ type 1 receptor (TGFBR1, ALK5) that then phosphorylates the transcription factors SMAD2 and 3 in what is referred to as the canonical pathway (Derynck and Zhang, 2003; Leask, 2010; Wynn, 2008). SMAD6 and 7 inhibit SMAD2 and 3 activity by competitively binding to TGFBR1 or by enhancing receptor degradation (Derynck and Zhang, 2003). TGFβ can also signal through non-canonical or SMAD-independent pathways that include the mitogen-activated protein kinase (MAPK) signaling branches, extracellular signal-regulated kinases (ERK), c-Jun N-terminal kinase (JNK), and p38 kinases. Both canonical and non-canonical signaling have been implicated in myofibroblast activation and fibrosis (Leask, 2010).

Transient receptor potential canonical (TRPC) family members can be transcriptionally induced and/or are directly activated by G-protein coupled-receptor (GPCR) signaling through diacylgylcerol, in addition to being more susceptible to opening with depletion of intracellular Ca^{2+} stores or by stretch of the plasma membrane (Eder & Molkentin, 2011). TRPC channel-mediated Ca^{2+} influx can directly activate the Ca^{2+}-sensitive protein phosphatase calcineurin to program diverse intracellular responses through its downstream transcriptional effector nuclear factor of activated T-cells (NFAT) (Kuwahara et al., 2006). TRPC6-calcineurin signaling has not been previously implicated in regulating myofibroblast transformation or tissue fibrosis, although one intriguing study suggested that endothelin-1 (ET-1) dependent upregulation of TRPC6 via $Ga_{12/13}$ signaling actually inhibited myofibroblast formation despite ET-1 being a profibrotic ligand (Nishida et al., 2007). While not associated with fibrosis, TRPC6 expression and/or activity has been implicated in podocyte cytoskeletal remodeling (Wang et al., 2009), human keratinocyte differentiation (Woelfle et al., 2010), and hippocampal neuron differentiation (Wu et al., 2004).

RESULTS

TRPC6 promotes fibroblast to myofibroblast transdifferentiation

To identify regulators of myofibroblast transdifferentiation we utilized the mammalian genome collection of expressed cDNAs (expression plasmids) to perform a cell-based gain-of-function screen in SV40 transformed mouse embryonic fibroblasts (MEFs). We utilized an αSMA-luciferase promoter plasmid as a transcriptional-program surrogate for myofibroblast activation. Less than 1% of 18,400 full-length cDNAs screened elicited a signal greater or equal to that obtained with recombinant TGFβ treatment. Two of the positive cDNAs identified were the known fibroblast activator interleukin-6 (IL6) and TRPC6 (Figure 1A). We confirmed the fibroblast-activating effect with a second luciferase reporter plasmid containing the periostin (*Postn*) promoter, which is also induced in

transformed fibroblasts. TRPC6 overexpression induced both reporters similar to TGFβ treatment (Figure 1A).

To investigate if TRPC6 can directly induce fibroblast to myofibroblast transdifferentiation we infected MEFs, primary rat cardiac fibroblasts and primary human dermal fibroblasts with a recombinant adenovirus (Ad) expressing TRPC6 or Adβgal (control) and then assayed for αSMA stress fiber formation and collagen I by confocal microscopy 48 hrs later (Figure 1B and 1C). AdTRPC6 infection induced αSMA stress fiber positivity and conversion of approximately 50% of all three types of fibroblasts, in a manner similar to TGFβ or AngII treatment, while less than 5% of control fibroblasts expressed αSMA (Figure 1C). AdTRPC6 infection also enhanced expression of the myofibroblast specific ED-A isoform of fibronectin by western blotting (Fn-EDA, Figure 1D). As myofibroblasts contract a collagen gel matrix (Rice and Leinwand, 2003; Tomasek et al., 2002), AdTRPC6 infected fibroblasts or TGFβ treated showed contraction over 36 hrs while Adβgal infected controls did not (Figure 1E and 1F). However, the contraction of collagen gel matrices induced by TRPC6 overexpression was not due to altered cardiac fibroblast proliferation (Figure 1G).

TRPC channels form homo- or heterotetramers although overexpression of any one subunit alone can enhance Ca^{2+} currents (Eder and Molkentin, 2011). To determine if myofibroblast transformation was specific to TRPC6 we also evaluated the ability of AdTRPC3 and AdTRPC4 infection to induce αSMA expression and contract collagen matrices in primary cardiac fibroblasts (Figure S1A, S1B, and S1C). TRPC4 showed no effect while TRPC3 overexpression weakly converted some fibroblasts to myofibroblasts, although not nearly to the same magnitude as TRPC6.

Loss of TRPC6 prevents TGFβ-mediated myofibroblast transformation

To determine if TRPC6 is required for myofibroblast conversion, dermal fibroblasts isolated from *Trpc6* wildtype (Wt) and null littermates (Dietrich et al., 2005) were examined for TGFβ induction of αSMA stress fiber formation and contractile function. Remarkably, *Trpc6*−/− primary dermal fibroblasts showed no induction of αSMA positive stress fibers with TGFβ treatment in contrast to robust induction in similarly prepared Wt fibroblasts (Figure 2A). Moreover, TGFβ induced profound contraction of collagen gels cultured with Wt fibroblasts, while *Trpc6*−/− fibroblasts were refractory to TGFβ-mediated contraction (Figure 2B, and 2C). Interestingly, the ability to repopulate a scratched confluent monolayer in culture was either not impaired in *Trpc6*−/− fibroblasts or was more proficient compared with Wt fibroblasts, depending on culturing conditions (Figure 2D).

TRPC6 is necessary for dermal and cardiac wound healing

Here a dermal wound-healing model was employed in which 2 dorsal 6 mm punch biopsies were taken from *Trpc6* Wt and null littermates. Wounds were first generated in Wt mice and the healing border areas were dissected at day 4 for RT-PCR analysis of TRPC6 mRNA. TRPC6 mRNA was dramatically induced in the wounds from 3 separate mice compared with lower levels in 2 uninjured control mice (Figure 3A). Consistent with these results, *Trpc6*−/− mice had significantly impaired wound closure rates over time such that by day 5 when *Trpc6* Wt mice had highly retracted wounds, *Trpc6*−/− mice attained only 33.1% retraction (Figure 3B and 3C). At 3 days post biopsy the border zones of the wounds were stained for αSMA (myofibroblasts) and isolectin (endothelial cells) (Figure 3D). *Trpc6*−/− histological sections had significantly less myofibroblasts per area than Wt counterparts suggesting that the poor dermal wound healing in *Trpc6*−/− mice could be due to impaired myofibroblast formation (Figure 3D and 3E).

We also examined a cardiac injury model involving myocardial infarction (MI), as myofibroblast transformation is critical to maintain ventricular wall structural integrity and to reduce dilation. Compared with Wt mice, *Trpc6*^{−/−} mice had significantly higher rates of mortality due to ventricular wall rupture throughout 3–7 days post MI injury, a time during which scar formation and remodeling mostly occurs (Figure 3F). The *Trpc6*^{−/−} mice that survived MI had significantly smaller scar sizes, greater reductions in cardiac function, and significantly greater ventricular wall dilation compared with Wt MI mice (Figure 3G, 3H and 3I).

Non-canonical TGFβ signaling induces TRPC6 gene expression to activate myofibroblasts

TGFβ stimulation induced mRNA levels of TRPC6 in primary cardiac fibroblasts but not in other TRPC family members, except for a slight increase in TRPC1 (Figure 4A). Immunofluorescent analysis of cardiac fibroblasts fixed 48 hrs after TGFβ treatment also showed enhanced TRPC6 protein levels, similar to AdTRPC6 infection (Figure 4B). Since TGFβ can mediate its effects through canonical (SMAD2/3) or non-canonical (MAPK) pathways we examined these downstream effects. The TGFβ-dependent induction of TRPC6 expression was not inhibited by infection with AdSMAD6 or AdSMAD7, known inhibitors of canonical signaling (Figure 4C). However, the p38 MAPK inhibitor SB731445 completely blocked TGFβ-dependent induction of TRPC6 expression suggesting a critical role for non-canonical signaling in TRPC6 induction.

Signaling by p38 MAPK is elicited by many different inflammatory cytokines (not just TGFβ signaling), such as through AngII and its receptor, which also fully induced TRPC6 gene expression in a p38-dependent manner (Figure 4C). This was particularly interesting because p38 signaling might represent a common intracellular event in myofibroblast transformation between diverse inflammatory cytokines and their different receptors. Indeed, TGFβ mediated αSMA stress fiber positivity and myofibroblast transformation was inhibited by blockade of p38 signaling, but not by AdSMAD7 (Figure 4D and 4E).

Importantly, shRNA mediated knockdown of the ALK5 (TGFBRI) receptor that fully suppressed TGFβ-dependent myofibroblast transformation did not inhibit TRPC6-dependent transformation (Figure 4F). This result indicates that TRPC6 is downstream of the TGFβreceptor complex in mediating myofibroblast transformation, although it does not distinguish canonical versus non-canonical signaling. Finally, ALK5 deficient cardiac fibroblasts infected with AdMKK6, which purely drives p38 MAPK signaling, fully promoted αSMA positive stress fiber formation and myofibroblast transformation, similar to AngII treatment, indicating that non-canonical p38 mobilization is the critical aspect of TGFβ signaling in forming myofibroblasts. This result also explains how AngII, ET-1 and select other inflammatory cytokines can themselves drive myofibroblast transformation without eliciting TGFβ signaling or SMAD transcriptional responses (see discussion).

SRF directly induces TRPC6 gene expression downstream of TGFβ-p38 MAPK signaling

SRF and its transcriptional cofactors, myocardin and myocardin-related transcription factor (MRTF), are activated by TGFβ receptor signaling to facilitate αSMA gene expression and myofibroblast transformation (Chai et al., 2007; Crider et al., 2011; Sandbo et al., 2009). Investigation of the mouse TRPC6 proximal promoter (−1187 to +1) identified several potential SRF binding sites, of which the most proximal promoter sequence at −123 to −114 was highly conserved (Benson et al., 2011). Here we determined that SRF overexpression in fibroblasts, but not the related transcription factor myocyte enhancer factor 2a (MEF2a), upregulated TRPC6 mRNA expression, which was blocked with the p38 inhibitor SB731445 (Figure 5A). Transfection of a luciferase reporter plasmid containing a 1187 base pair TRPC6 proximal promoter showed induction by TGFβ, SRF, and synergistic activation

with both together (Figure 5B). A TRPC6 promoter deletion construct (−215) containing the conserved proximal SRF binding site (CArG box) at −123 to −114, showed over 3-fold induction with TGFβ stimulation, yet an identical promoter construct with this site mutated was unresponsive to TGFβ (Figure S2A). The induction of TRPC6 promoter activity by SRF was blocked with the p38 inhibitor (Figure 5B). Importantly, chromatin immunoprecipitation (ChIP) experiments spanning −1238 to −855 bp of the TRPC6 promoter showed SRF binding that was induced with TGFβ but reduced with an adenovirus expressing an shRNA against SRF, suggesting direct regulation of TRPC6 gene expression (Figure 5C). Indeed, ChIP with an anti-phospho-SRF antibody (activated SRF) showed even greater inducible occupancy of the TRPC6 promoter upon TGFβ stimulation (Figure 5C). Similar results were achieved by ChIP with another primer pair that amplified the most proximal CArG element near the start site of transcription (data not shown). Gel shift analysis of the proximal −123 CArG box showed optimal binding of SRF from cell extracts that was blocked with prior infection with a recombinant adenovirus expressing an shRNA against SRF (Figure S2B). Collectively, these results suggest that SRF can bind and directly regulate the TPRC6 promoter in a p38 dependent manner.

AdSRF infection of primary Wt dermal fibroblasts fully induced myofibroblast transdifferentiation, as shown by immunocytochemistry for αSMA (Figure 5D and 5E). However, $Trpc6^{-/-}$ dermal fibroblasts were completely refractory to SRF-mediated induction of myofibroblast transdifferentiation, indicating that TRPC6 is a required downstream mediator of SRF-dependent myofibroblast transformation (Figure 5D and 5E). $Trpc6^{-/-}$ primary dermal fibroblasts were also refractory to TGFβ and AngII-mediated myofibroblast transdifferentiation, cytokines that are known to induce SRF or MRTF activity (Martin-Garrido et al., 2011; Small et al., 2010) (Figure 5E).

Finally, to examine the necessity of SRF in mediating TGFβ or AngII-dependent myofibroblast transdifferentiation we used a recombinant adenoviral construct expressing an shRNA against SRF (Streb and Miano, 2005). Knock-down of SRF (>80% by western blot, (Figure 5F)) prevented both TGFβ and AngII-dependent myofibroblast transdifferentiation, but importantly, it did not inhibit transdifferentiation mediated by AdTRPC6 as assessed by αSMA staining or gel contraction assays (Figure 5G and 5H). Ad-shSRF infection of primary fibroblasts also reduced baseline TRPC6 mRNA expression, as well as blocked TGFβ induction of expression (Figure S2C). These results place SRF in a critical intermediary position in the transdifferentiation signaling cascade, where it receives input from TGFβ and other profibrotic cytokines through p38 MAPK signaling, which then directly mediates TRPC6 gene expression to mobilize a Ca^{2+}-dependent pathway for transdifferentiation (see below).

TGFβ-p38 signaling enhances Ca^{2+} through TRPC6 in activated myofibroblasts

Given TRPC6's role in Ca^{2+} entry, cardiac fibroblasts were either treated with TGFβ or infected with AdTRPC6 for 48 hrs and then SOCE was measured. Representative traces and quantification of the intracellular Ca^{2+} signal showed significant increases with AdTRPC6 and with 48 hrs of TGFβ and AngII compared to no treatment (Figure 6A and Figure S3A). This increase in SOCE was not due to acute TGFβ signaling since 15 minutes of ligand treatment had no effect, suggesting it was likely mediating transcriptional changes.

Relative to Wt dermal fibroblasts that demonstrated a nearly 2-fold increase in SOCE with TGFβ treatment, $Trpc6^{-/-}$ fibroblasts had no change, indicating that TRPC6 is the primary mediator of the TGFβ-dependent enhancement of SOCE in activated fibroblasts (Figure 6B). Moreover, this TGFβ-dependent increase in SOCE in fibroblasts was significantly reduced with a p38 MAPK inhibitor, while unitary activation of p38 with AdMKK6 infection induced a small, albeit significant increase in SOCE (Figure 6C). These results

support the overall signaling model whereby non-canonical TGFβ signaling through p38 enhances myofibroblast transformation through a Ca^{2+} signal that uniquely depends on *Trpc6* gene expression. However, these results do not establish that SOCE is the mechanism behind TRPC6's ability to convert fibroblasts (SOCE was simply a surrogate assay for TRPC function), as TRPC channels can also mediate Ca^{2+} influx independent of store depletion (see discussion).

TRPC6-dependent Ca^{2+} induces calcineurin-NFAT for myofibroblast transformation

TRPC channels mediate their biologic effects primarily through Ca^{2+} influx and Ca^{2+}-dependent signaling effectors, of which calcineurin-NFAT has been particularly implicated (Kuwahara et al., 2006). Indeed, nearly 50% of cardiac fibroblasts infected with a recombinant adenovirus expressing a constitutively active calcineurin (ΔCnA) mutant showed αSMA positive stress fibers similar to TRPC6 overexpression (Figure 6D and 6E). Coinfection of TRPC6 with the calcineurin-NFAT inhibitor Cain fully blocked this conversion while Cain alone had no effect (Figure 6D and 6E). Moreover, inhibition of calcineurin with Cain or specific inhibition of only NFAT with VIVIT blocked myofibroblast formation and collagen gel contraction in cardiac fibroblasts stimulated with TGFβ or AdTRPC6 (Figure S3B). *Ppp3r1* (calcineurin B1) null MEFs (lack all calcineurin activity) were also unable to contract a collagen gel after TGFβ or AdTRPC6 infection (Figure S3C). Taken together, these results indicate that activation of calcineurin is sufficient to drive myofibroblast transdifferentiation and that calcineurin signaling is necessary for TRPC6- and TGFβ-dependent formation of myofibroblasts.

TRPC6 overexpression caused a 12-fold increase in NFAT activity (Figure 6F) that could be blocked by Cain (*data not shown*). AdΔCnA was used as a positive control yielding a 50-fold induction of NFAT activity (Figure 6F). TGFβ also elicited a significant increase in NFAT activity, although it was only 2-fold above baseline (Figure 6F). A more sensitive assay involving NFAT translocation showed a remarkable association between NFAT and TRPC6/TGFβ signaling. Specifically, NFATc1-GFP normally resides in both the cytoplasm and nucleus of quiescent fibroblasts, while infection with AdΔCnA sends all the NFATc1-GFP to the nucleus (Figure 6G). Both TGFβ and TRPC6 specifically sent essentially all of the NFATc1-GFP to the nucleus only in those fibroblasts that had converted to myofibroblasts with αSMA positivity (Figure 6G). Placing this result within the hierarchy of the larger signaling pathway, we also observed that AdΔCnA-induced myofibroblast transformation was independent of p38 MAPK since the inhibitor did not reduce αSMA positivity (Figure 6E). Moreover, inhibition of SRF with an shRNA against SRF did not block the ability AdΔCnA to induce myofibroblast transdifferentiation (Figure 5G). Finally, TGFβ stimulation also increased expression of calcineurin Aβ mRNA levels, which enhances total calcineurin activity (Figure S3D and S3E).

Wt or *Trpc6*$^{-/-}$ fibroblasts infected with AdΔCnA each showed robust gel contraction, similar to AdTRPC6 infection (Figure 7A and 7B). As a control, TGFβ was still unable to elicit contraction in collagen gels containing *Trpc6*$^{-/-}$ fibroblasts (Figure 2B and 7B). Collectively, these results indicate that calcineurin-NFAT signaling is downstream of the TGFβ-p38 MAPK-SRF signaling event that mediates enhanced TRPC6 expression/activity. These results define the ability of calcineurin to drive myofibroblast transformation as the downstream mediator or TRPC6 induction.

The TRPC6-calcineurin-NFAT signaling axis is necessary for dermal wound healing

Since ΔCnA overcame the defect in myofibroblast collagen gel contraction with loss of *Trpc6*, we hypothesized that activated calcineurin would restore defective wound healing in *Trpc6*$^{-/-}$ mice. To examine this hypothesis AdΔCnA, AdTRPC6 or AdGFP (as an internal

control) was topically applied to dermal punch biopsies in Wt and *Trpc6*$^{-/-}$ mice (Figure 7C). AdΔCnA significantly improved the rate of wound closure in *Trpc6*$^{-/-}$ mice at each designated time point, similar to or even slightly better than AdTRPC6, while AdGFP infection had no effect (Figure 7C and 7D). Consistent with this result, *Ppp3c*$^{-/-}$ (calcineurin Aβ) mice had significantly impaired dermal wound closure rates at days 4–7, although by day 10 healing eventually caught up to Wt controls (Figure 7E). Similarly, Wt mice treated with tacrolimus (FK506), a calcineurin inhibitor, showed a mild but significant impairment in wound healing, as previously suggested in the literature (Gisquet et al., 2011; Schaffer et al., 1998) (data not shown). By comparison, *Trpc6*$^{-/-}$ mice had a more profound wound closure defect that never resolved even up to 10 days post injury (Figure 7E).

DISCUSSION

Here we discovered a previously unrecognized function for TRPC6-calcineurin-NFAT signaling in myofibroblast transformation and wound healing *in vivo*. This TRPC6-calcineurin-NFAT pathway is mobilized by p38 MAPK, a nodal stress-induced and proinflammatory signaling effector that functions downstream of non-canonical TGFβ signaling and other GPCR agonists that mediate fibrosis (Figure 7F). This profibrotic cytokine signaling pathway mobilizes the transcriptional activity of SRF, which in turn mediates myofibroblast transdifferentiation through its ability to specifically upregulate TRPC6 gene expression. The most profound observation of our study was that singular activation of TRPC6 or calcineurin fully mediates myofibroblast transformation without TGFβ or other profibrotic cytokines, as well as without SRF. Moreover, loss of *Trpc6* fully inhibited myofibroblast transformation *in vitro*, regardless of the stimulating profibrotic ligand used or if SRF was overexpressed. We also demonstrated that calcineurin-NFAT is necessary for TRPC6-mediated Ca^{2+} influx in programming myofibroblast transformation (Figure 7F). NFAT has been shown to regulate αSMA expression in activated pulmonary myofibroblasts (Rice and Leinwand, 2003). Also, αSMA, fibronectin and collagen gene expression can all be activated by NFAT signaling (Cobbs and Gooch, 2007; Gonzalez Bosc et al., 2005; Lejard et al., 2007).

Role of non-canonical signaling and p38 MAPK in myofibroblast transformation

Myofibroblast transformation is elicited by an array of inflammatory ligands (TGFβ, ET-1, IL6, AngII, etc) and also by mechanical stretch (Hinz, 2007; Leask, 2010; Tomasek et al., 2002). However, the vast majority of the literature in this area is dominated by the role that canonical SMAD2/3-dependent TGFβ signaling has in facilitating myofibroblast transformation (Hinz., 2007; Leask, 2010). In our current study inhibition of canonical signaling with SMAD6 or SMAD7 had no effect on myofibroblast transformation or TRPC6 expression downstream of TGFβ, but inhibition of non-canonical p38 signaling fully blocked TGFβ-TRPC6-dependent myofibroblast transformation. These data are consistent with previous work in fibroblasts in which TGFβ induced a prolonged activation of p38 MAPK signaling that increased collagen, fibronectin, and αSMA expression (Kim et al., 2007; MeyerD-Ter-Vehn et al., 2006). In fact, TGFβ-mediated induction of αSMA stress fibers was blocked in MEFs by deleting the downstream p38 target MK2 (MAPK-activated protein kinase 2) (Sousa et al., 2007). Similar results were obtained in glomerular mesangial cells when the upstream activator of p38, MKK3, was overexpressed causing the expression of myofibroblast target genes (Wang et al., 2002).

The conventional paradigm is that AngII requires TGFβ signaling to induce collagen production and fibrosis (Rosenkranz, 2004). However, in our studies ALK5 knockdown in cardiac fibroblasts did not block AngII-mediated myofibroblast transformation (Figure 4F). There are two potential hypotheses to explain this result. First, AngII could activate noncanonical p38 signaling through secretion of TGFβ that signals through TGFBR2 or

second, AngII could directly activate p38 MAPK signaling through a GPCR pathway that is then fully capable of initiating myofibroblast transformation through p38-TRPC6-calcineurin-NFAT. There is supportive evidence for the later hypothesis since TGFβ neutralizing antibodies are unable to block AngII induction of myofibroblast markers (Leask, 2010) and *Tgfbr1* deficient hearts with pressure overload still activate non-canonical p38 signaling to drive cardiac remodeling (Koitabashi et al., 2011). Similarly AngII in this study acted like TGFβ in promoting TRPC6 gene expression and Ca^{2+} entry, which were both effectively blocked with a p38 inhibitor.

Role of TRPC6, Ca^{2+} influx and calcineurin

That enhanced Ca^{2+} influx elicits downstream myofibroblast transformation is consistent with reports of Ca^{2+} driving both differentiation and cytoskeletal rearrangement in other cell types (Wang et al., 2009; Woelfle et al., 2010). However, in human atrial fibroblasts isolated from atrial fibrillation patients there was a higher level of myofibroblast differentiation due to increased Ca^{2+} influx, albeit through the upregulation of a different TRP family channel, TRPM7 (transient receptor potential melastatin 7; Mg^{2+} and Ca^{2+} entry) (Du et al., 2010). This study actually supports our current results since TRP family members can hetero-oligomerize between families (Alessandri-Haber et al., 2009; Ma et al., 2010), so it is possible that select TRPC and TRPM family members generate complexes that mediate physiologic Ca^{2+} entry for myofibroblast transformation.

The elevated SOCE attained from increased TRPC6 expression provides an ample Ca^{2+} signal to activate calcineurin-NFAT signaling (Figure S3A). However, this does not imply that SOCE is the mechanism behind TRPC6-mediated myofibroblast conversion, as TRPC channels can cause Ca^{2+} entry in response to receptor activation, stretch, and even other stress stimuli that do not involve changes in intracellular Ca^{2+} stores. We simply measured SOCE in our current study as an experimental surrogate for total TRPC6 "potential" for Ca^{2+} influx. While our results showing that TRPC6-calcineurin-NFAT mediate myofibroblast transformation have not been previously reported, work in the heart and other tissues has shown that calcineurin-NFAT signaling is activated by TRPC6 for other cellular functions (Kuwahara et al., 2006; Wu et al., 2010). Our data are most consistent with TRPC6 directly providing Ca^{2+} in a local microenvironment to calcineurin at the plasma membrane or in complex between calcineurin-TRPC6 in mediating activation, as inhibition of Inositol 1,4,5-trisphosphate (IP3) signaling with the IP3-sponge did not affect TRPC6-dependent conversion of myofibroblasts (data not shown).

If NFAT is involved as the primary mediator of calcineurin-induced myofibroblast transformation, it probably functions in accord with other transcriptional regulators, such as SRF and the MRTFs (co-regulators of SRF), and possibly SMAD proteins. Indeed, mice lacking the MRTF-A protein were defective in myofibroblast conversion and scar formation after MI injury (Small et al., 2010). Notably, in an *in vitro* epithelial-mesenchymal transition model, MRTF-dependent activation of αSMA transcription required p38 signaling (Sebe et al., 2008) suggesting a cooperative relationship between p38 signaling and MRTF induction of fibrotic genes and myofibroblast function.

In summary these findings define a role for TRPC6-calcineurin-NFAT signaling as a molecular circuit for myofibroblast transformation and tissue repair. The identification of this signaling arm offers an additional avenue for developing targeted intervention points in fibrotic diseases. While calcineurin is unlikely to be a therapeutic target given all the signaling inputs it receives from other Ca^{2+} influx pathways, as well as its highly diverse biologic functions, TRPC6 appears more dedicated to this cellular differentiation mechanism and inhibitors could be developed to reduce its activity.

EXPERIMENTAL PROCEDURES

Dermal wound healing assay and topical adenoviral application

For the dermal wound-healing model mice underwent anesthesia, their backs were prepared and two 6 mm excisional wounds were created with a disposable biopsy punch (Integra Miltex) on either side of the dorsal midline. Wounds were measured and photographed daily in order to assess wound retraction and health. In some experiments biopsies were made and topically treated with the following adenoviral vectors for 15 minutes before applying a Tegaderm adhesive which held the virus in the wounded area. Wound photographs were analyzed by ImageJ software (NIH) to measure surface areas.

Myocardial infarction and echocardiography

To create myocardial infarcts (MI) 10-week old mice were subjected to permanent occlusion of the left coronary artery after a thoracotomy procedure where the left coronary artery was ligated with 8-0 suture. M-mode echocardiography (Hewlett Packard SONOS 5500) was performed in anesthetized mice with a 15-MHz transducer at 3 and 7 days after MI surgery to assess cardiac function and ventricular geometry anesthesia.

TGFβ/AngII treatments, adenoviral gene transfer and shRNA lentiviral knockdown

Application of recombinant porcine TGFβ (10 ng/ml, R&D System) or AngII (100 nM, Sigma) was used to induce myofibroblast transformation. The p38 inhibitor (SB731445) was delivered in 50 nM doses. For experiments that required adenoviral gene transfer, fibroblasts were incubated in adenovirus for 24 hrs at which time the media was changed and the cells were typically incubated for an additional 24–48 hrs. For knockdown of the SRF gene rat cardiac fibroblasts were adenovirally transduced with short hairpin (sh) RNA constructs shGFP (control) or shSRF. At two days post shSRF/shGFP gene transfer fibroblasts were adenovirally infected with AdTRPC6 or AdΔCnA or pharmacologically treated with TGFβ (10 ng/ml) or AngII (100 nM). For knockdown of the ALK5 gene (TGFβ-receptor 1, NM_009370) Mission shRNA lentivirus (Sigma, TRCN0000022479, 80, 81, 82, 83) was obtained and knockdown was achieved at 4 days post gene transfer.

TRPC6 luciferase reporter and luciferase assay

Three DNA fragments, −215 to +1, −215 to +1 with a mutated CArG site, and 1187 to +1, of the murine TRPC6 promoter were individually subcloned into the *XhoI* and *HindIII* sites of the pGL3 promoter luciferase plasmid (Promega) to make TRPC6 reporter constructs. The proximal and highly conserved consensus CArG site at −123 (5' CCTTTAAAGG 3') in the TRPC6 promoter was mutated to TGTGCGAAGG (Genewiz Inc.). For luciferase assays rat cardiac fibroblasts were maintained in media + 1% serum and transiently cotransfected with a TRPC6 luciferase reporter (Mirus, Trans-IT) and either a βgal or SRF plasmid. In addition some transfected fibroblasts were also treated with TGFβ (10 ng/ml) or p38 inhibitor (50 nM). Luciferase activity was measured 48 hours post transfection.

Collagen gel contraction assay

Fibroblasts at 70% confluence were adenovirally infected if experimentally required or grown in culture media for 24 hrs. Fibroblasts were harvested from a confluent monolayer by Trypsin-EDTA digestion (0.25%), pelleted and resuspended in DMEM with 1% serum. Fibroblasts were then seeded into collagen matrices such that each gel contained 40,000 fibroblasts and cast in 24-well plates. The collagen gels were released from the edges and floating in DMEM with 1% serum. ImageJ software (NIH) was used to calculate the surface area, which are reported as values normalized to the initial size of the gel.

Statistical Tests

Statistical significance was determined by ANOVA and Newman-Keuls pairwise comparisons for multivariate experiments and t-test for experiments with 2 groups.

Supplementary Material

Refer to Web version on PubMed Central for supplementary material.

Acknowledgments

REFERENCES

Alessandri-Haber N, Dina OA, Chen X, Levine JD. TRPC1 and TRPC6 channels cooperate with TRPV4 to mediate mechanical hyperalgesia and nociceptor sensitization. J Neurosci. 2009; 29:6217–6228. [PubMed: 19439599]

Benson CC, Zhou Q, Long X, Miano JM. Identifying functional single nucleotide polymorphisms in the human CArGome. Physiol Genomics. 2011; 43:1038–1048. [PubMed: 21771879]

Chai J, Norng M, Tarnawski AS, Chow J. A critical role of serum response factor in myofibroblast differentiation during experimental oesophageal ulcer healing in rats. Gut. 2007; 56:621–630. [PubMed: 17068115]

Cobbs SL, Gooch JL. NFATc is required for TGFbeta-mediated transcriptional regulation of fibronectin. Biochem Biophys Res Commun. 2007; 362:288–294. [PubMed: 17719012]

Crider BJ, Risinger GM Jr, Haaksma CJ, Howard EW, Tomasek JJ. Myocardin-Related Transcription Factors A and B Are Key Regulators of TGF-beta1-Induced Fibroblast to Myofibroblast Differentiation. J Invest Dermatol. 2011; 131:2378–2385. [PubMed: 21776010]

Derynck R, Zhang YE. Smad-dependent and Smad-independent pathways in TGF-beta family signalling. Nature. 2003; 425:577–584. [PubMed: 14534577]

Dietrich A, Mederos YSM, Gollasch M, Gross V, Storch U, Dubrovska G, Obst M, Yildirim E, Salanova B, Kalwa H, et al. Increased vascular smooth muscle contractility in TRPC6-/- mice. Mol Cell Biol. 2005; 25:6980–6989. [PubMed: 16055711]

Du J, Xie J, Zhang Z, Tsujikawa H, Fusco D, Silverman D, Liang B, Yue L. TRPM7-mediated Ca2+ signals confer fibrogenesis in human atrial fibrillation. Circ Res. 2010; 106:992–1003. [PubMed: 20075334]

Eder P, Molkentin JD. TRPC channels as effectors of cardiac hypertrophy. Circ Res. 2011; 108:265–272. [PubMed: 21252153]

Gisquet H, Liu H, Blondel WC, Leroux A, Latarche C, Merlin JL, Chassagne JF, Peiffert D, Guillemin F. Intradermal tacrolimus prevent scar hypertrophy in a rabbit ear model: a clinical, histological and spectroscopical analysis. Skin Res Technol. 2011; 17:160–166. [PubMed: 21241368]

Gonzalez Bosc LV, Layne JJ, Nelson MT, Hill-Eubanks DC. Nuclear factor of activated T cells and serum response factor cooperatively regulate the activity of an alphaactin intronic enhancer. J Biol Chem. 2005; 280:26113–26120. [PubMed: 15857835]

Hinz B. Formation and function of the myofibroblast during tissue repair. J Invest Dermatol. 2007; 127:526–537. [PubMed: 17299435]

Kim SI, Kwak JH, Zachariah M, He Y, Wang L, Choi ME. TGF-betaactivated kinase 1 and TAK1-binding protein 1 cooperate to mediate TGF-beta1-induced MKK3-p38 MAPK activation and stimulation of type I collagen. Am J Physiol Renal Physiol. 2007; 292:F1471–F1478. [PubMed: 17299140]

Koitabashi N, Danner T, Zaiman AL, Pinto YM, Rowell J, Mankowski J, Zhang D, Nakamura T, Takimoto E, Kass DA. Pivotal role of cardiomyocyte TGF-beta signaling in the murine

pathological response to sustained pressure overload. J Clin Invest. 2011; 121:2301–2312. [PubMed: 21537080]

Kuwahara K, Wang Y, McAnally J, Richardson JA, Bassel-Duby R, Hill JA, Olson EN. TRPC6 fulfills a calcineurin signaling circuit during pathologic cardiac remodeling. J Clin Invest. 2006; 116:3114–3126. [PubMed: 17099778]

Leask A. Potential therapeutic targets for cardiac fibrosis: TGFbeta, angiotensin, endothelin, CCN2, and PDGF, partners in fibroblast activation. Circ Res. 2010; 106:1675–1680. [PubMed: 20538689]

Lejard V, Brideau G, Blais F, Salingcarnboriboon R, Wagner G, Roehrl MH, Noda M, Duprez D, Houillier P, Rossert J. Scleraxis and NFATc regulate the expression of the pro-alpha1(I) collagen gene in tendon fibroblasts. J Biol Chem. 2007; 282:17665–17675. [PubMed: 17430895]

Ma X, Qiu S, Luo J, Ma Y, Ngai CY, Shen B, Wong CO, Huang Y, Yao X. Functional role of vanilloid transient receptor potential 4-canonical transient receptor potential 1 complex in flow-induced Ca2+ influx. Arterioscler Thromb Vasc Biol. 2010; 30:851–858. [PubMed: 20093626]

Martin-Garrido A, Brown DI, Lyle AN, Dikalova A, Seidel-Rogol B, Lassegue B, San Martin A, Griendling KK. NADPH oxidase 4 mediates TGF-beta-induced smooth muscle alpha-actin via p38MAPK and serum response factor. Free Radic Biol Med. 2011; 50:354–362. [PubMed: 21074607]

Meyer-Ter-Vehn T, Gebhardt S, Sebald W, Buttmann M, Grehn F, Schlunck G, Knaus P. p38 inhibitors prevent TGF-beta-induced myofibroblast transdifferentiation in human tenon fibroblasts. Invest Ophthalmol Vis Sci. 2006; 47:1500–1509. [PubMed: 16565385]

Nishida M, Onohara N, Sato Y, Suda R, Ogushi M, Tanabe S, Inoue R, Mori Y, Kurose H. Galpha12/13-mediated up-regulation of TRPC6 negatively regulates endothelin-1-induced cardiac myofibroblast formation and collagen synthesis through nuclear factor of activated T cells activation. J Biol Chem. 2007; 282:23117–23128. [PubMed: 17533154]

Rice NA, Leinwand LA. Skeletal myosin heavy chain function in cultured lung myofibroblasts. J Cell Biol. 2003; 163:119–129. [PubMed: 14557251]

Rosenkranz S. TGF-beta1 and angiotensin networking in cardiac remodeling. Cardiovasc Res. 2004; 63:423–432. [PubMed: 15276467]

Sandbo N, Kregel S, Taurin S, Bhorade S, Dulin NO. Critical role of serum response factor in pulmonary myofibroblast differentiation induced by TGF-beta. Am J Respir Cell Mol Biol. 2009; 41:332–338. [PubMed: 19151320]

Schaffer MR, Fuchs N, Proksch B, Bongartz M, Beiter T, Becker HD. Tacrolimus impairs wound healing: a possible role of decreased nitric oxide synthesis. Transplantation. 1998; 65:813–818. [PubMed: 9539093]

Sebe A, Masszi A, Zulys M, Yeung T, Speight P, Rotstein OD, Nakano H, Mucsi I, Szaszi K, Kapus A. Rac, PAK and p38 regulate cell contact-dependent nuclear translocation of myocardin-related transcription factor. FEBS Lett. 2008; 582:291–298. [PubMed: 18154735]

Serini G, Bochaton-Piallat ML, Ropraz P, Geinoz A, Borsi L, Zardi L, Gabbiani G. The fibronectin domain ED-A is crucial for myofibroblastic phenotype induction by transforming growth factor-beta1. J Cell Biol. 1998; 142:873–881. [PubMed: 9700173]

Small EM, Thatcher JE, Sutherland LB, Kinoshita H, Gerard RD, Richardson JA, Dimaio JM, Sadek H, Kuwahara K, Olson EN. Myocardin-related transcription factor-a controls myofibroblast activation and fibrosis in response to myocardial infarction. Circ Res. 2010; 107:294–304. [PubMed: 20558820]

Sousa AM, Liu T, Guevara O, Stevens J, Fanburg BL, Gaestel M, Toksoz D, Kayyali US. Smooth muscle alpha-actin expression and myofibroblast differentiation by TGFbeta are dependent upon MK2. J Cell Biochem. 2007; 100:1581–1592. [PubMed: 17163490]

Streb JW, Miano JM. AKAP12alpha, an atypical serum response factordependent target gene. J Biol Chem. 2005; 280:4125–4134. [PubMed: 15590635]

Tomasek JJ, Gabbiani G, Hinz B, Chaponnier C, Brown RA. Myofibroblasts and mechano-regulation of connective tissue remodelling. Nat Rev Mol Cell Biol. 2002; 3:349–363. [PubMed: 11988769]

Wang L, Ma R, Flavell RA, Choi ME. Requirement of mitogen-activated protein kinase kinase 3 (MKK3) for activation of p38alpha and p38delta MAPK isoforms by TGF-beta 1 in murine mesangial cells. J Biol Chem. 2002; 277:47257–47262. [PubMed: 12374793]

Wang Z, Wei X, Zhang Y, Ma X, Li B, Zhang S, Du P, Zhang X, Yi F. NADPH oxidase-derived ROS contributes to upregulation of TRPC6 expression in puromycin aminonucleoside-induced podocyte injury. Cell Physiol Biochem. 2009; 24:619–626. [PubMed: 19910702]

Woelfle U, Laszczyk MN, Kraus M, Leuner K, Kersten A, Simon-Haarhaus B, Scheffler A, Martin SF, Muller WE, Nashan D, et al. Triterpenes promote keratinocyte differentiation in vitro, ex vivo and in vivo: a role for the transient receptor potential canonical (subtype) 6. J Invest Dermatol. 2010; 130:113–123. [PubMed: 19675576]

Wu X, Eder P, Chang B, Molkentin JD. TRPC channels are necessary mediators of pathologic cardiac hypertrophy. Proc Natl Acad Sci U S A. 2010; 107:7000–7005. [PubMed: 20351294]

Wu X, Zagranichnaya TK, Gurda GT, Eves EM, Villereal ML. A TRPC1/TRPC3-mediated increase in store-operated calcium entry is required for differentiation of H19-7 hippocampal neuronal cells. J Biol Chem. 2004; 279:43392–43402. [PubMed: 15297455]

Wynn TA. Cellular and molecular mechanisms of fibrosis. J Pathol. 2008; 214:199–210. [PubMed: 18161745]

Highlights

- TRPC6 induction can fully induce fibroblast to myofibroblast transformation

- Loss of TRPC6 blocks myofibroblast transformation to TGFβ and fibrotic cytokines

- Calcineurin-NFAT signaling is necessary and sufficient for myofibroblast formation

- TRPC6-Calcineurin-mediated myofibroblast conversion utilizes p38MAPK and SRF activity

In Brief (eTOC blurb)

Fibroblasts transdifferentiate into myofibroblasts in response to cytokines; myofibroblasts mediate tissue repair and fibrosis. Davis et al. show that the Ca^{2+} channel TRPC6 and Ca^{2+}-activated phosphatase calcineurin are necessary and sufficient for myofibroblast differentiation, downstream of a TGFβ signaling pathway that utilizes p38 MAPK and the transcription factor SRF.
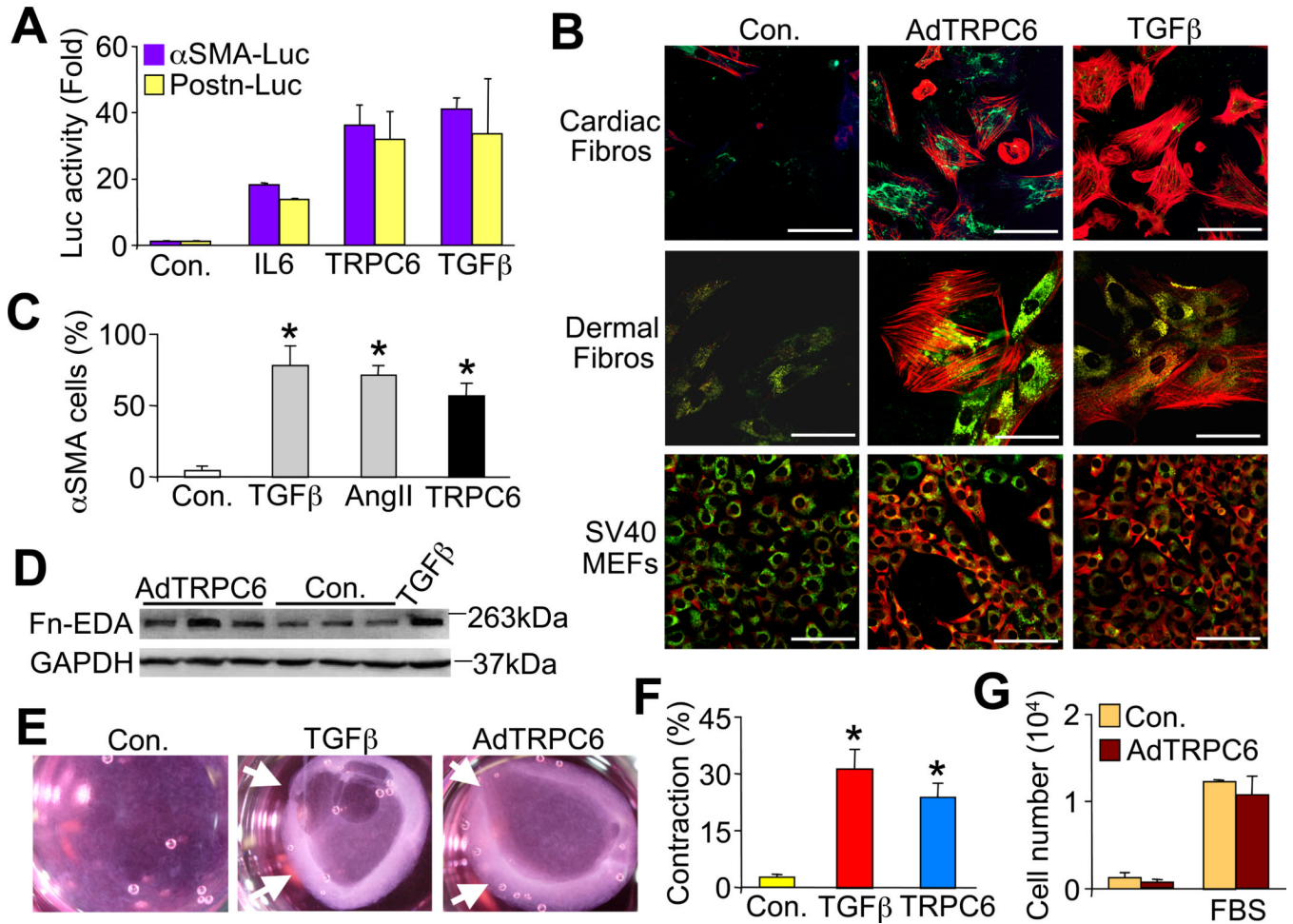
Figure 1.
TRPC6 overexpression promotes fibroblast to myofibroblast conversion. (**A**) αSMA-luciferase and Postn-luciferase promoter activity from cultured neonatal rat cardiac fibroblasts transfected with expression vectors encoding TRPC6 or IL6, or treated with recombinant TGFβ(−/−). (**B**) Immunofluorescent staining of αSMA (red) positive stress fibers and collagen I (green) in 3 different fibroblast cell lines infected with adenovirus (Ad) encoding TRPC6 or stimulated with recombinant TGFβ. Scale bar is 50 μm. (**C**) Quantification of the experiment shown in **B**, except that cardiac fibroblasts were used, as was AngII treatment (100 nM). N 700 cells per group. Control (Con.) represents Adβgal infection or no drug. *P<0.05 vs control. (**D**) Western blot for fibronectin ED-A in AdTRPC6 infected versus uninfected control cardiac fibroblasts (GAPDH serves as a loading control). (**E**) Photographs and (**F**) quantification of floating collagen gel matrices seeded with cardiac fibroblasts that have contracted after 36 hrs of TGFβ or AdTRPC6 infection. *P<0.05 vs. control; N=3 independent experiments. Arrows in E show area of gel contraction. (**G**) Cardiac fibroblast proliferation measured by colormetric MTT (tetrazoleum) assay 48 hrs after AdTRPC6 or Adβgal (con.) infection in serum-free or medium containing 10% fetal bovine serum (FBS). N=3 independent experiments. All data represent the mean ± s.e.m (error bars).
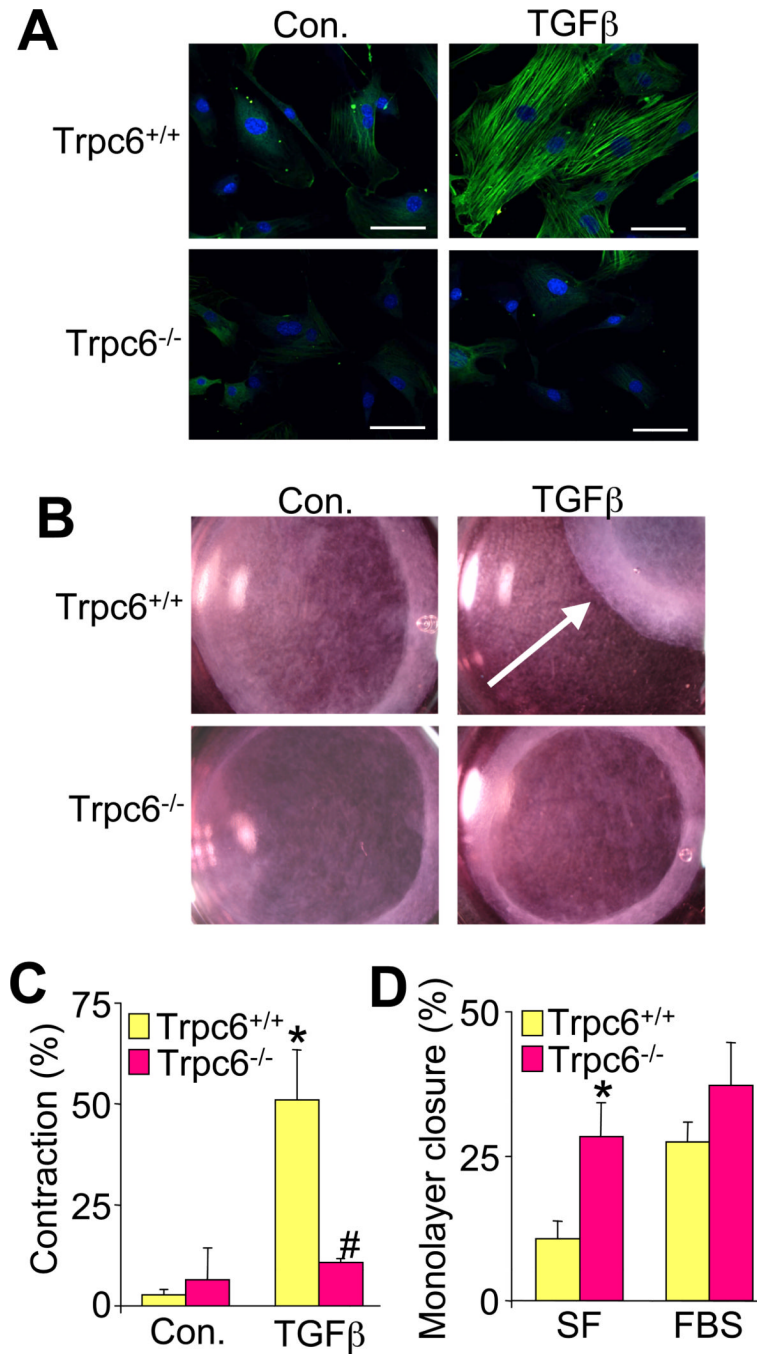
Figure 2.
Loss of TRPC6 prevents TGFβ-mediated myofibroblast conversion. (**A**) Immunofluorescent staining of αSMA (green) positive stress fibers and TOPRO-3 iodide nucleic acid stain (blue) in primary *Trpc6⁺/⁺* (Wt) and *Trpc6⁻/⁻* dermal fibroblasts, with and without recombinant TGFβ stimulation. Scale bar is 50 μm. (**B**) Photographs and (**C**) quantification of contraction of floating collagen gel matrices seeded with *Trpc6⁺/⁺* or *Trpc6⁻/⁻* dermal fibroblasts at 36 hours post TGFβ. *P<0.05 vs. control; #P<0.05 vs. *Trpc6⁺/⁺* with TGFβ; N=3. The arrow in B shows contraction of the gel. (**D**) Quantification of *in vitro* scratch closure rates in *Trpc6⁺/⁺* and *Trpc6⁻/⁻* fibroblast monolayers in culture in serum free and

10% fetal bovine serum conditions (FBS). The scratch area was measured at time 0 and 24 hours later. *P<0.05 vs. $Trpc6^{+/+}$; N=3. All data represent the mean ± s.e.m (error bars).
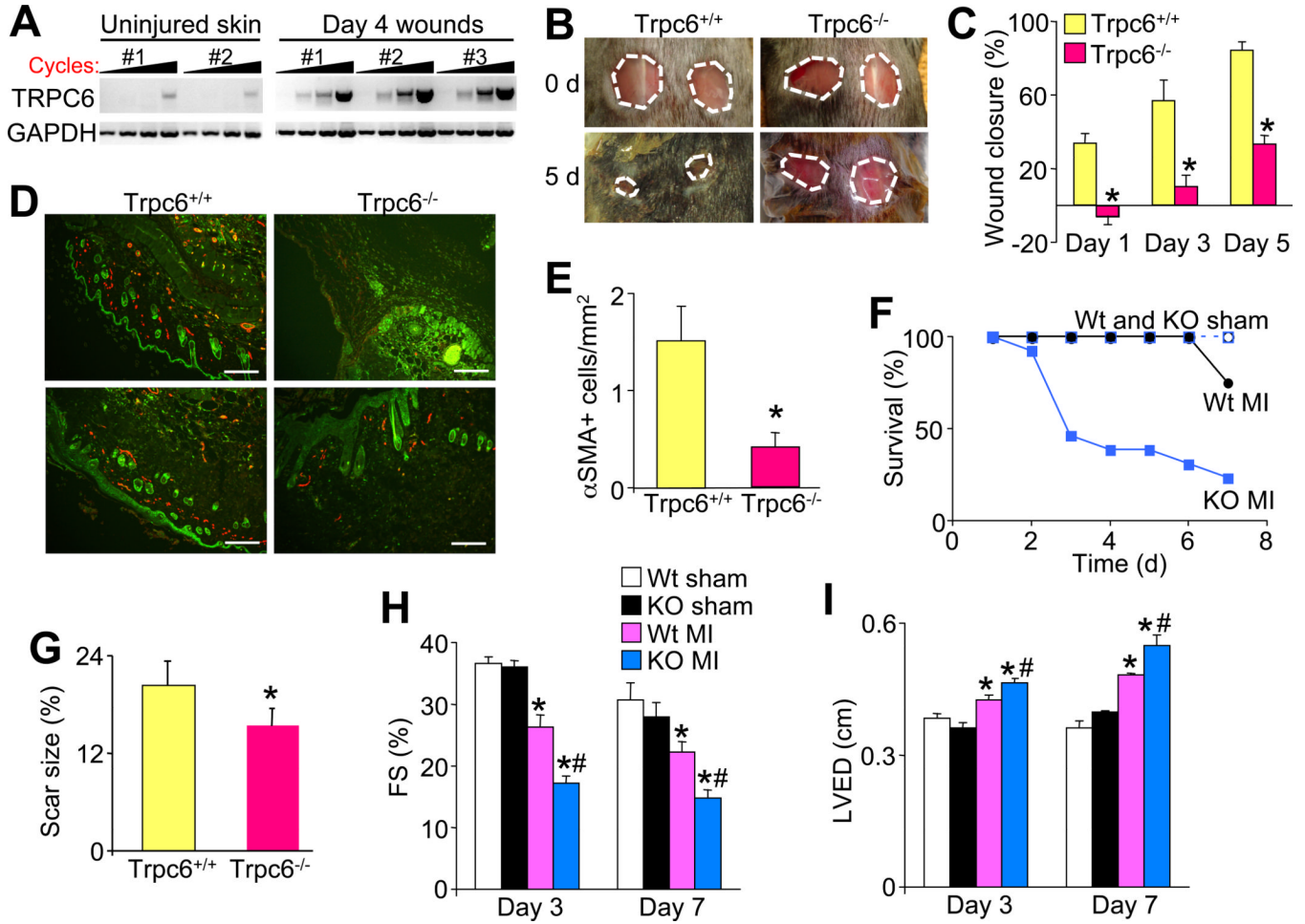
Figure 3.
TRPC6 is necessary for dermal and cardiac wound healing. (**A**) RT-PCR for TRPC6 mRNA from skin wounds of 3 separate mice or uninjured skin of 2 control mice. GAPDH is used as a control. (**B**) Photographs of 2 full excision 6 mm dorsal coat (skin) punch biopsies taken on 8–10 week old *Trpc6*$^{+/+}$ and *Trpc6*$^{−/−}$ littermates at day 0, and the progression shown again at day 5. (**C**) Quantification of dermal would closure rates. N=8 per group. *P<0.05 vs *Trpc6*$^{+/+}$. (**D** and **E**) Wound border zone pictures and quantitation at 3 days post biopsy stained with isolectin (green) to detect epithelial tissue and αSMA (red) to detect myofibroblasts, which was quantified. Scale bar = 0.1 mm. *P<0.05 vs *Trpc6*$^{+/+}$; N=4 per group. (**F**) Survival curves of *Trpc6*$^{+/+}$ (Wt) and *Trpc6*$^{−/−}$ (KO) littermates after sham or permanent coronary ligation surgery (MI). (**G**) Quantification of scar size at 1-week post coronary ligation in surviving *Trpc6*$^{+/+}$ and *Trpc6*$^{−/−}$ mice. *P<0.05 vs *Trpc6*$^{+/+}$; N=5 per group. (**H, I**) M-mode echocardiographic assessment of left ventricular fractional shortening (FS %) and left ventricular end diastolic dimensions (LVED) in the indicated groups of mice. *P<0.05 vs Wt sham; #P<0.05 vs Wt MI; N=10–14 per group. All data represent the mean ± s.e.m (error bars).
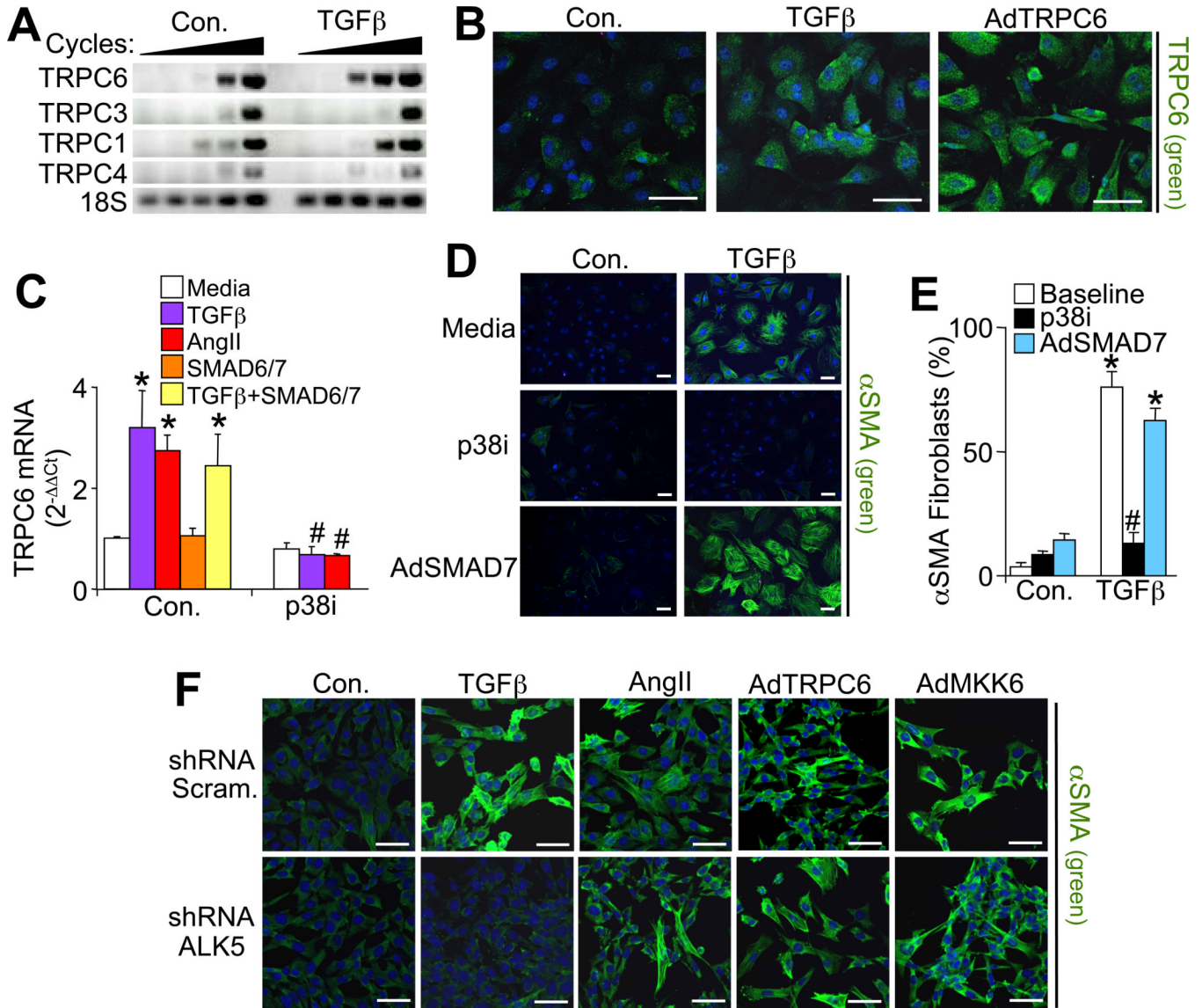
Figure 4.
Non-canonical TGFβ-mediated signaling induces TRPC6 gene expression to activate myofibroblasts. (**A**) Representative RT-PCR for TRPC family members in which PCR product was sampled every 5 cycles starting at cycle 20 from cardiac fibroblasts ± 12 hours of TGFβ treatment. (**B**) Immunofluorescent staining of TRPC6 (green) and TOPRO-3 iodide nucleic acid stain (blue) in cardiac fibroblasts treated with TGFβ or infected with AdTRPC6. Scale bar is 50 μm. (**C**) Real time PCR for TRPC6 induction (*normalized to 18sRNA*) from cardiac fibroblasts that were simultaneously treated for 24 hours with profibrotic molecules (TGFβ or AngII) ± non-canonical (p38 inhibitor, SB731445) or canonical (adenoviral SMAD6/7) inhibitors. *P<0.05 vs media; #P<0.05 vs control with same treatment; N=3 independent experiments run in duplicate. (**D**) Immunofluorescent staining and (**E**) quantification of αSMA (green) positive stress fibers and TOPRO-3 iodide nucleic acid stain (blue) in cardiac fibroblasts that were treated for 48 hours with TGFβ. Some groups also received non-canonical (p38 inhibitor, SB731445) or canonical (AdSMAD7 infection) inhibitors as depicted. *P<0.05 vs control; #P<0.05 vs baseline with same treatment; N 250 cells per group over 2 independent experiments. Scale bar is 50 μm.

(**F**) Immunofluorescent staining of αSMA expression (green) in fibroblasts expressing a scrambled shRNA control or shRNA-anti-ALK5 that were also treated with TGFβ, AngII or infected with AdTRPC6, or AdMKK6. Nuclei are shown in blue. Scale bar is 50 μm. All data represent the mean ± s.e.m (error bars).
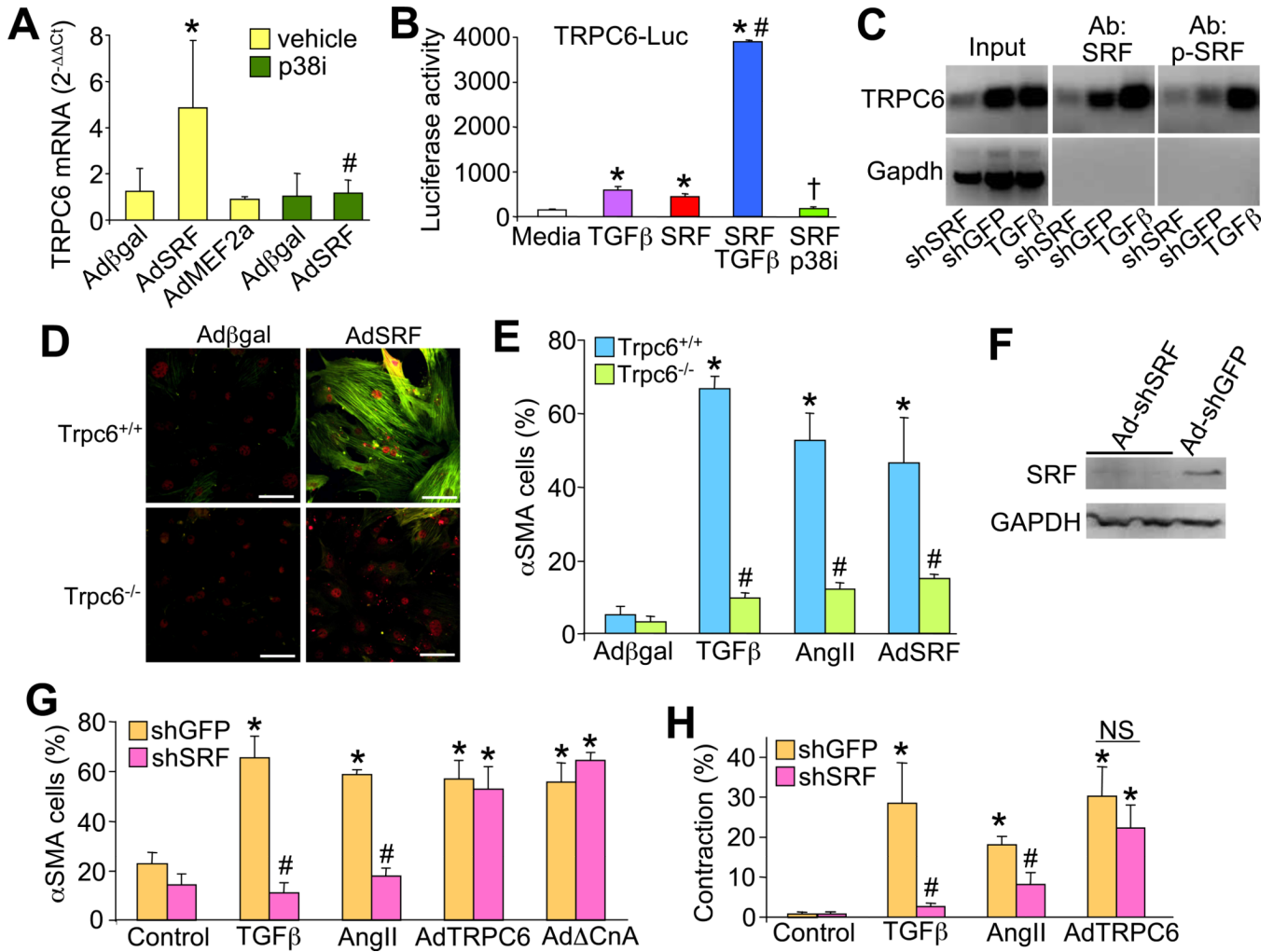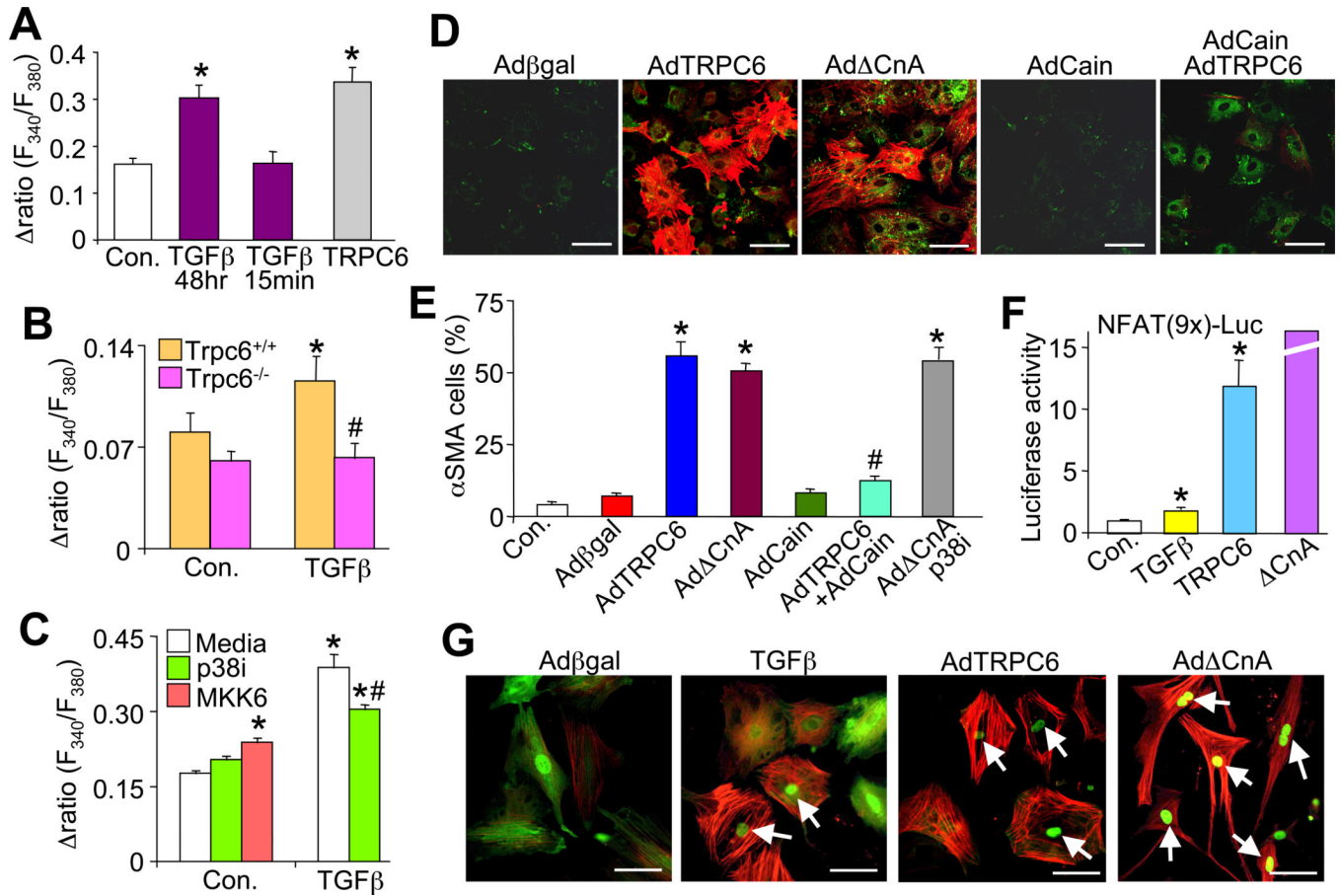
Figure 5.
SRF mediates TRPC6 gene expression and myofibroblast transdifferentiation. (**A**) Real time PCR analysis of TRPC6 mRNA in primary cardiac fibroblasts infected with the indicated adenoviruses, with or without p38 inhibitor (SB731445). *P<0.05 vs Adβgal; #P<0.05 vs AdSRF + vehicle. Results are averaged from 3 independent experiments. (**B**) TRPC6-luciferase promoter activity (-1187 bp) from fibroblasts co-transfected with the indicated plasmids or treated with TGFβ or SB731445. *P<0.05 vs media (untransfected); #P<0.05 versus TGFβ or SRF; †P<0.05 vs SRF alone. (**C**) ChIP assay from the TRPC6 promoter regions (−1238 to −855 bp) for SRF using a standard or phospho-specific SRF antibody. Cells were previously treated with or without TGFβ or infected with Ad-shSRF or Ad-shGFP as a control. (**D**) Immunocytochemistry for αSMA (green) in Wt or *Trpc6−/−* primary dermal fibroblasts infected with Adβgal or AdSRF. Red staining is SRF. Scale bar is 50 μm. (**E**) Quantitation of percentage of αSMA converted Wt or *Trpc6−/−* fibroblasts treated with the agonist or adenovirus shown. (N=3 experiments; *P<0.05 vs Adβgal Wt; #P<0.05 vs Wt of the same treatment). (**F**) Western blot for SRF or GAPDH in fibroblasts infected with AdshSRF or Ad-shGFP control. (**G**) Immunocytochemistry for αSMA (green) or (**H**) collagen gel contraction assays in control (shGFP) or shSRF adenoviral infected primary dermal fibroblasts treated with TGFβ, AngII, or co-infected with the indicated adenoviruses. Scale bar is 50 μm. (N=3 experiments; *P<0.05 vs control; #P<0.05 vs shGFP of the same co-treatment. NS = not significant). All data represent the mean ± s.e.m (error bars).

Figure 6.
TRPC6-mediated Ca^{2+} signaling mediates myofibroblast transdifferentiation. (**A**)
Quantification of store-operated calcium entry (SOCE) for control (no treatment or Adβgal
infection, N=24), TGFβ treated (N=25), and AdTRPC6 (N=54) infected cardiac fibroblasts.
*P<0.05 vs control; 3 independent experiments were performed. (**B**) Quantification of
SOCE in $Trpc6^{+/+}$ and $Trpc6^{-/-}$ dermal fibroblasts ± 48 hr TGFβ treatment. *P<0.05 vs
control $Trpc6^{+/+}$; #P<0.05 vs TGFβ in $Trpc6^{+/+}$ fibroblasts; N 20 cells per group derived
from 3 independent experiments. (**C**) Quantification of SOCE from control (N=159), TGFβ
treated (N=71), and AdTRPC6 (N=41) infected cardiac fibroblasts ± p38 inhibitor (N=32) or
± AdMKK6 (N=32). *P<0.05 vs media under control conditions; #P<0.05 vs TGFβ with
media; consisting of over 3 independent experiments. SOCE is calculated as the difference
between the peak Ca^{2+} signal obtained during Ringer's reperfusion and the steady-state Ca^{2+}
level reached after CPA treatment. (**D**) Immunofluorescent staining and (**E**) quantification of
αSMA (red) positive stress fibers and collagen I (green) in cardiac fibroblasts 48 hrs post
adenoviral infection with Adβgal, AdTRPC6, AdΔCnA, AdCain (calcineurin-NFAT
inhibitor), or coinfection with AdTRPC6 + AdCain. *P<0.05 vs Adβgal; #P<0.05 vs
AdTRPC6; N 750 cells per group from 2 independent experiments. (**F**) N-luciferase activity
from cardiac fibroblasts infected with the reporter AdNFATx9-Luc, AdTRPC6, AdΔCnA or
treated with recombinant TGFβ. *P<0.05 vs control; N=3 independent experiments. (**G**)
Immunofluorescent staining of αSMA (red) positive stress fibers and the localization of
NFAT-GFP in cardiac fibroblasts coinfected with AdNFATc1-GFP and AdTRPC6,
AdΔCnA, or treated with TGFβ. Arrows indicate fibroblasts that have αSMA stress fibers
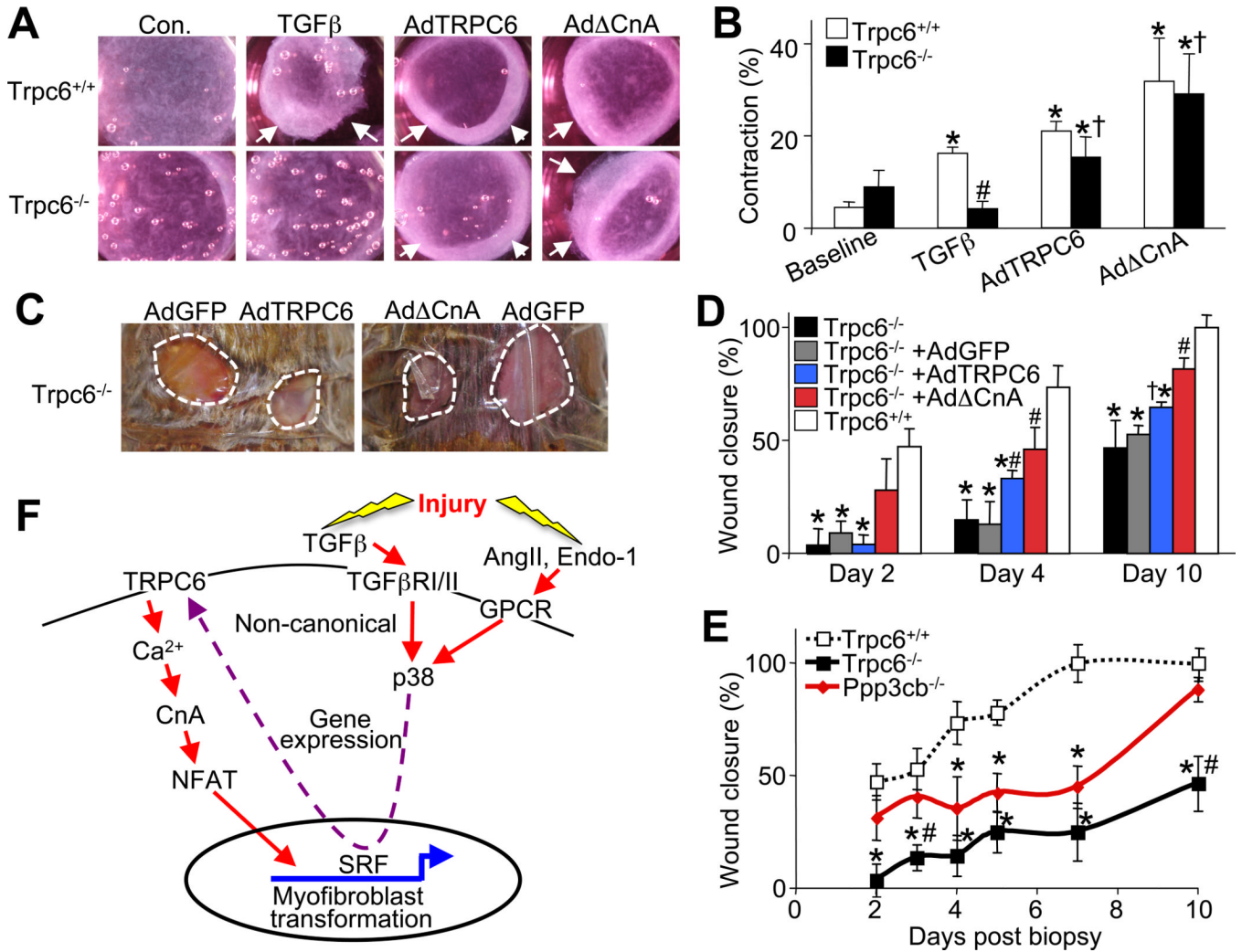and NFAT in the nucleus. All data represent the mean ± s.e.m (error bars).

Figure 7.
The TRPC6-Calcineurin-NFAT signaling axis is necessary for dermal wound healing. (**A**) Photographs and (**B**) quantification of floating collagen gel matrix contraction rates seeded prior with $Trpc6^{+/+}$ or $Trpc6^{-/-}$ dermal fibroblasts at 48 hrs post infection with AdTRPC6, AdΔCnA, or treated with recombinant TGFβ. Arrows indicate the contracted diameter of the collagen matrix. *P<0.05 vs. baseline; #P<0.05 vs. $Trpc6^{+/+}$ TGFβ; †P<0.05 vs. TGFβ in $Trpc6^{-/-}$; N=3 independent experiments. (**C**) Photographs of 2 full excision 6 mm dorsal dermal punch biopsies taken on 8–10 week old $Trpc6^{+/+}$ or $Trpc6^{-/-}$ littermates 4 days after the biopsy. Topical application of adenovirus containing GFP, TRPC6 or ΔCnA was applied to the site just after wounding. (**D**) Time course of wound closure for $Trpc6^{-/-}$ mice compared with $Trpc6^{+/+}$ controls and treated with the indicated adenovirus. N=8 mice per group. *P<0.05 vs $Trpc6^{+/+}$ (Wt); #P<0.05 vs $Trpc6^{-/-}$ AdGFP; †P<0.05 vs $Trpc6^{-/-}$ alone or $Trpc6^{-/-}$ AdGFP. (**E**) Time course of wound closure for $Trpc6^{+/+}$, $Trpc6^{-/-}$, or $Ppp3cb^{-/-}$ mice. N=8 per group. *P<0.05 vs $Trpc6^{+/+}$ (Wt); #P<0.05 vs $Ppp3cb^{-/-}$. (**F**) Signaling model for myofibroblast transdifferentiation whereby non-canonical TGFβ signaling cascade through p38 signaling to SRF, mediates a transcriptional upregulation of TRPC6 gene expression, enhancing Ca^{2+} entry leading to calcineurin (CnA) activation, sending NFAT to the nucleus to participate in myofibroblast phenotypic conversion. All data represent the mean ± s.e.m (error bars).